Applied Physics Letters ARTICLE scitation.org/journal/apl

Origins of hydrogen that passivates bulk defects in silicon heterojunction solar cells

Cite as: Appl. Phys. Lett. **115**, 252103 (2019); doi: 10.1063/1.5132368
Submitted: 17 October 2019 · Accepted: 5 December 2019 ·
Published Online: 17 December 2019

Chang Sun,[1,a)] William Weigand,[2] Jianwei Shi,[2] Zhengshan Yu,[2] Rabin Basnet,[1] Sieu Pheng Phang,[1] Zachary C. Holman,[2] and Daniel Macdonald[1]

AFFILIATIONS

[1]Research School of Electrical, Energy and Materials Engineering, The Australian National University, Canberra, ACT 2601, Australia
[2]School of Electrical, Computer, and Energy Engineering, Arizona State University, Tempe, Arizona 85287, USA

[a)]Author to whom correspondence should be addressed: chang.sun@anu.edu.au

ABSTRACT

Silicon heterojunction solar cell fabrication incorporates a significant amount of hydrogen into the silicon wafer bulk, and the amount of injected hydrogen is comparable to that introduced by silicon nitride films during a high-temperature firing step. In this work, the origins of the hydrogen injected during heterojunction cell processing have been identified. We demonstrate that the hydrogen plasma treatment that is routinely included to improve surface passivation considerably increases the hydrogen concentration in the wafers. We also show that the hydrogenated amorphous silicon i/p^+ stack is more effective than the i/n^+ stack for bulk hydrogen incorporation, and both are more effective than intrinsic films alone.

Hydrogen is known to passivate a wide range of defects and impurities in silicon, including grain boundaries, dislocations, and many pointlike deep levels.[1,2] Such passivation usually improves the performance of silicon solar cells and is thus of great interest to the photovoltaic industry.[1–6] A common hydrogen source in homojunction solar cells is a plasma-enhanced chemical vapor deposited (PECVD) hydrogenated silicon nitride (SiN_x:H) film, which introduces hydrogen into the bulk during a fast firing step typically at 700–800 °C used for contact formation.[7,8] In a previous study,[9] we demonstrated that significant hydrogen can also be incorporated into the cell bulk at <250 °C in silicon heterojunction (SHJ) cells and that the incorporated hydrogen concentration [H] is comparable to that introduced by firing SiN_x:H films. However, the responsible structure or treatment for this low-temperature bulk hydrogen incorporation remains unknown. This phenomenon is likely related to the hydrogen effusion from the hydrogenated amorphous silicon (a-Si:H) films, which were frequently investigated in previous studies.[10–14] In this work, we aim to further identify the origins of hydrogen for the bulk defect passivation in SHJ cells.

To identify the origins of hydrogen, various structures of lifetime samples were prepared in this work, and the regeneration rate of the boron-oxygen-related (BO) defect in those structures was determined. The positive correlation between the regeneration rate of BO defects and bulk hydrogen concentration [H] has been shown in numerous studies.[7–9,15–19] In Ref. 17, different firing peak temperatures, firing times, and cooling rates were applied on SiN_x:H-passivated samples to create different [H]. The regeneration rate of BO defects was found to positively correlate with the expected [H]. Therefore, in this work, we use the regeneration rate of BO defects as an indicator of [H]. For consistency with our previous study,[9] wafers from an *n*-type upgraded metallurgical-grade (UMG) Czochralski (Cz) silicon ingot supplied by Apollon Solar were used.[20] The boron and phosphorus concentrations were $[B] = 1.3 \times 10^{16}\,cm^{-3}$ and $[P] = 2 \times 10^{16}\,cm^{-3}$, as measured by secondary ion mass spectrometry. The control wafers were *n*-type electronic-grade (EG) Cz wafers with $[P] = 5 \times 10^{15}\,cm^{-3}$, as determined by dark conductance measurements. All the wafers were chemically etched, followed by Tabula Rasa and phosphorus gettering prefabrication treatments.[6] The interstitial oxygen concentrations in the UMG wafers were $[O_i] = 6–7 \times 10^{17}\,cm^{-3}$, as determined by Fourier transform infrared (FTIR) spectrophotometry.[6] After removing the phosphorus-diffused layers, the wafers were textured. The thicknesses of the UMG wafers and the EG wafers were about 130 μm and 260 μm, respectively. The following structures were prepared:

1. SiN_x:H-passivated, nonfired, and fired structures. A 70-nm-thick PECVD SiN_x:H film was deposited on each side at 300 °C, in a

Roth and Rau AK400 chamber. The fired samples were fired at 600 °C for 5 s in a rapid thermal annealing tool after the deposition. The fired films were then etched off and the samples were recoated with fresh SiN_x:H films.[9]

2. SHJ cell structure with no indium tin oxide (ITO) film or metallization: the $i/n^+ + i/p^+$ structure. An i/n^+ stack consisting of an 8-nm-thick a-Si:H (i) layer and a 4-nm-thick phosphorus-doped a-Si:H (n^+) layer was deposited on one side, and then an i/p^+ stack consisting of an 8-nm-thick a-Si:H (i) layer and 11-nm-thick boron-doped a-Si:H (p^+) layer was deposited on the other side, using an Applied Materials P-5000 multichamber PECVD tool. An *in situ* 15-s H_2 plasma treatment was performed after the deposition of a-Si:H (i), before the deposition of the doped films on each side. The H_2 plasma treatment is a part of the standard SHJ cell process, mainly to improve the a-Si:H (i)/crystalline silicon interface passivation.[21] The temperature of both the deposition and the H_2 plasma treatment was 250 °C.
3. The $i/n^+ + i/p^+$ structure with 70-nm-thick ITO films deposited on each side using DC magnetron sputtering.
4. The $i/n^+ + i/p^+$ structure without H_2 plasma treatments.

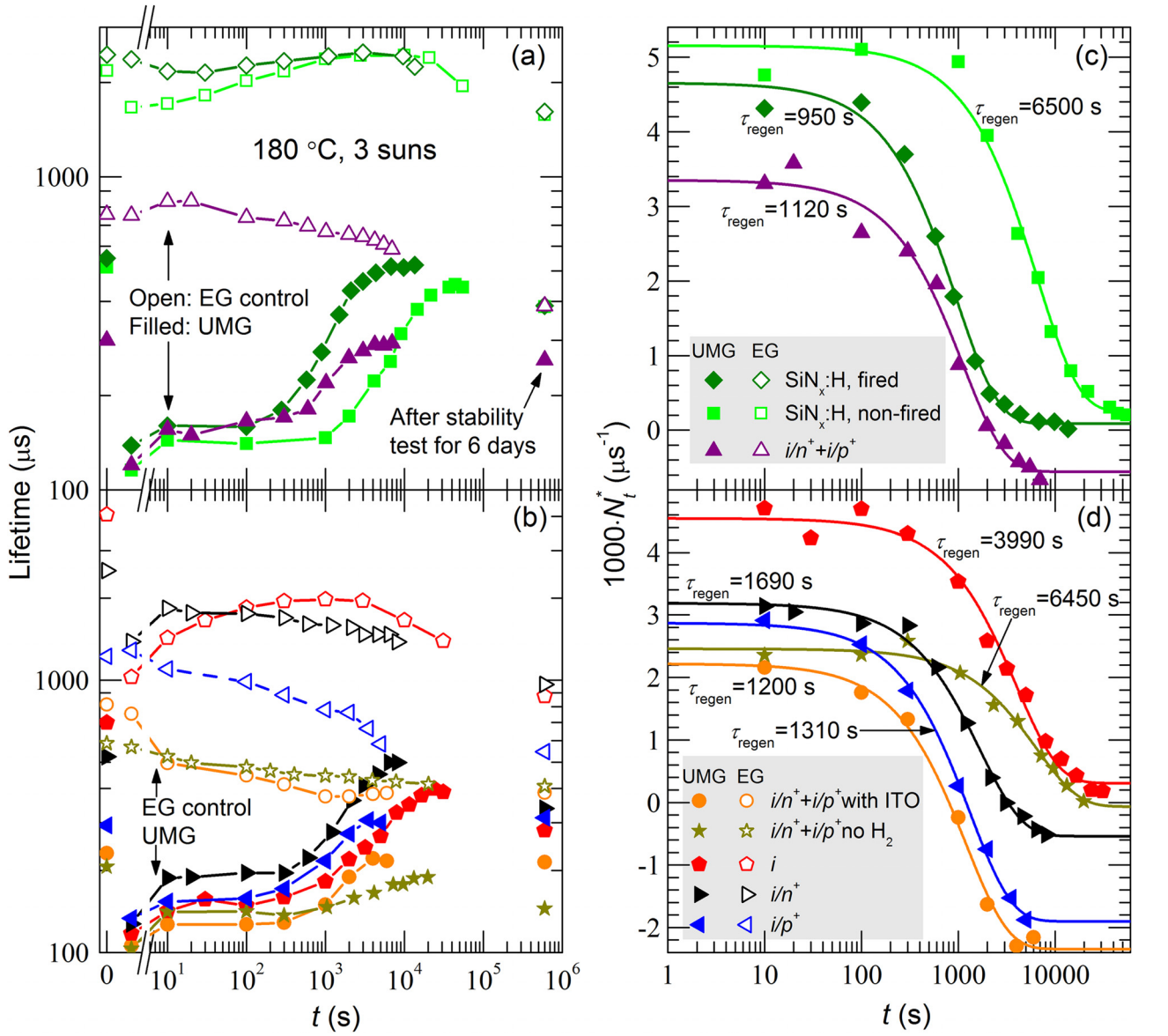

FIG. 1. Evolution of (a), (b) lifetime, and (c), (d) relative defect concentration during the regeneration of lifetime samples with various structures. The lines in (a) and (b) are guides to the eye, and the lines in (c) and (d) are exponential fits to Eq. (2) with the corresponding regeneration time constants shown in the plots. In (a) and (b), points at 0 s were measured after dark annealing, points before the axis break were measured after light soaking, and points at close to 10^6 s were measured after the stability test.

5. Symmetric a-Si:H (i) structure. Each side of the wafer was passivated with a 10-nm-thick a-Si:H (i) film followed by the H_2 plasma treatment.
6. Symmetric i/n^+ stack structure. The same i/n^+ stack as used in the second structure (with H_2 plasma treatment) was deposited on each side.
7. Symmetric i/p^+ stack structure. The same i/p^+ stack as used in the second structure (with H_2 plasma treatment) was deposited on each side.

To determine the regeneration rate of BO defects, the samples were first annealed in the dark at 200 °C for 20 min, to simulate the paste-curing step that occurs after screen printing in the SHJ cell fabrication,[5] as well as deactivating possibly activated BO defects. The lifetime after dark annealing, $\tau(0)$, was regarded as the background lifetime at $t = 0$, which is not affected by BO defects. The samples were then subjected to light soaking under 1 sun at 40–45 °C for 6 days,[9] before the regeneration under 3 suns at 180 °C until the lifetime saturates. A stability test under 1 sun at 40–45 °C for 6 days was performed after regeneration. The illumination in these processes was provided by a halogen lamp and measured by a reference cell.[22] Lifetime measurements were conducted periodically during the processes with a WCT-120 photoconductance lifetime tester, *ex situ* at room temperature. The carrier mobilities in compensated silicon, which are required input in the QSSPC software to calculate lifetimes, were calculated using the model in Ref. 23.

The regeneration kinetics of all structures are shown in Fig. 1. Lifetime values at $\Delta n = 0.1 n_0$ are reported and were used to extract the relative defect concentrations (inverse recombination lifetime of the defect), N_t^*. The change in the lifetime of the EG samples was mainly due to the instability of the SiN_x:H and a-Si:H films during illumination or annealing.[14,24] The EG control samples in Fig. 1 reveal that a-Si:H (i) layers and i/n^+ stacks provide better and more stable passivation than i/p^+ stacks. References 13 and 14 have reported the same observation on these films during dark annealing and explained that the i/p^+ stack releases more H_2, thus creating more Si dangling bonds upon annealing. The H_2 effusion from the films and the role of doping in facilitating the effusion will be discussed in greater detail later.

Assuming that (a) the effective lifetime of the EG control samples is dominated by the surface recombination and that (b) the same change in the surface recombination velocity occurs in the UMG and corresponding EG control samples, we calculate $N_t^*(t)$ as follows, to take into account of the change in the background lifetime of the UMG samples:[25]

$$N_t^*(t) = \left(\frac{1}{\tau_{UMG}(t)} - \frac{1}{\tau_{UMG}(0)}\right) - \frac{W_{EG}}{W_{UMG}}\left(\frac{1}{\tau_{EG}(t)} - \frac{1}{\tau_{EG}(0)}\right), \quad (1)$$

where W_{EG} and W_{UMG} are the thicknesses of the EG wafer and the UMG wafer. As shown in previous studies,[19,26] $N_t^*(t)$ during the regeneration can be fitted exponentially as follows:

$$N_t^*(t) = C_1 + C_2 \exp\left(-\frac{t}{\tau_{regen}}\right), \quad (2)$$

to obtain the regeneration rate constant τ_{regen}, as shown in Figs. 1(c) and 1(d). In Eq. (2), C_1 is the saturated defect concentration in the end of the regeneration and C_2 is the regenerated defect concentration. The regeneration rate R_{regen} is the inverse rate constant τ_{regen}^{-1}. The negative values of $N_t^*(t)$ in Figs. 1(c) and 1(d) may be indicating that there were active BO defects at $t = 0$ due to the incomplete deactivation of BO defects by the 200 °C dark annealing in this material.[27] However, this does not affect the extraction of the regenerations rates.

To use the regeneration rate as an indicator of [H], the correction of the injection level is required.[28] This is because different injection levels were achieved under the same 3-sun illumination due to different passivation qualities and optical properties of the films and stacks in these structures, and the regeneration rate is injection-dependent. For each UMG sample, the average injection level during the regeneration, $\Delta n_{average}$, was estimated (using lifetimes in the beginning and the end of regeneration) and used to correct R_{regen},[25,28] based on the relation $R_{regen} \propto \Delta n^{1.2}$ reported in Ref. 25. Figure 2 shows the corrected regeneration rates, which can be regarded as indicators of [H].

From Fig. 2, we can see that for SiN_x:H-passivated samples, the firing step significantly increases the corrected regeneration rate and therefore [H].[18] Even more [H] was incorporated into the $i/n^+ + i/p^+$ structure. These results confirm the conclusions of the previous study.[9] Comparing the $i/n^+ + i/p^+$ structure and its variations, we can also see that (1) the ITO does not impact [H] significantly. For this reason, we have included in Fig. 2 the symmetric i/n^+ with ITO and symmetric i/p^+ with ITO structures, to provide more statistics. (2) The H_2 plasma treatment considerably increases [H]. (3) Both i/n^+ and i/p^+ stacks inject more [H] than a-Si:H (i); the i/p^+ stack injects more [H] than i/n^+.

The second observation agrees with Ref. 21, which reported increased hydrogen concentration and SiH_2/SiH ratio (which will be discussed more) in a-Si:H(i) after the H_2 plasma treatment. The third observation might be partially explained by the different thicknesses: 10 nm for the a-Si:H(i) layers, 12 nm for the i/n^+ stack, and 19 nm for the i/p^+ stack. More importantly, as reported in Refs. 10–14, the

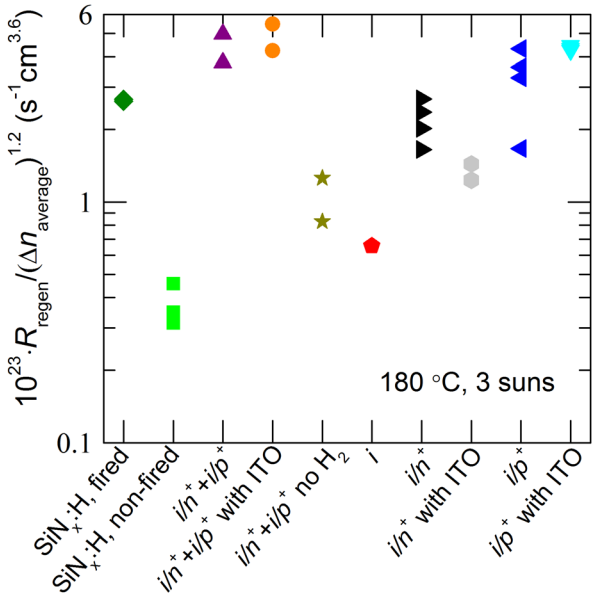

FIG. 2. Regeneration rates corrected with the average injection level. H_2 plasma treatment was conducted on all a-Si:H (i) films, alone or in a stack, unless otherwise mentioned.

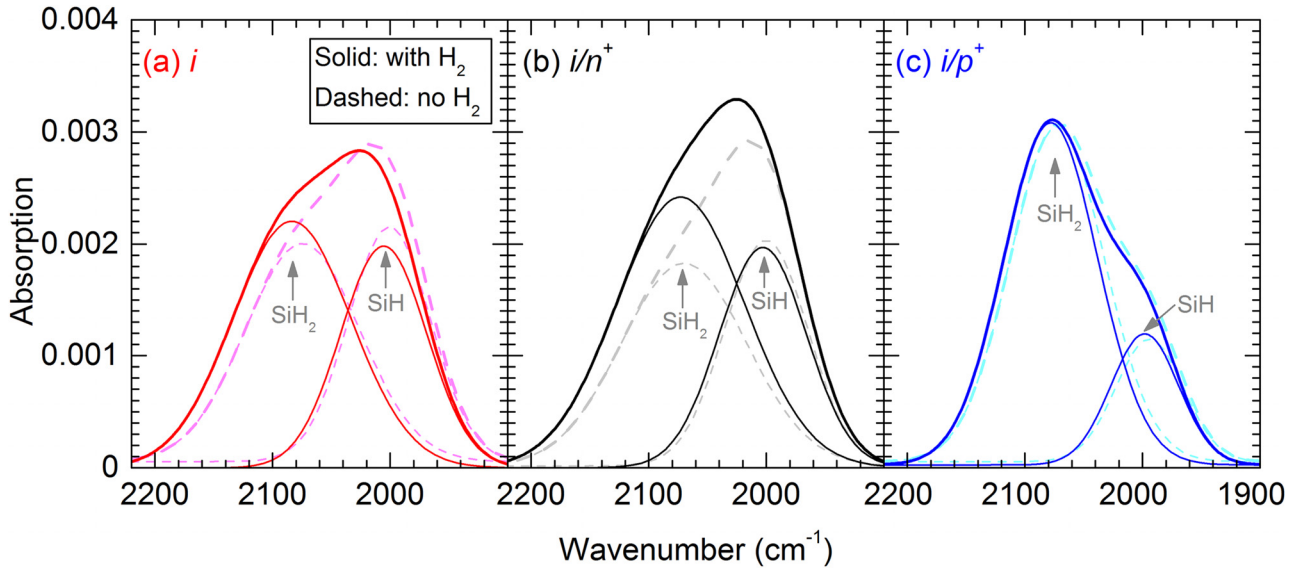

FIG. 3. FTIR absorption measured on wafers passivated with (a) a-Si:H(*i*) layers, (b) i/n^+ stacks, and (c) i/p^+ stacks, with and without H_2 plasma treatment.

doping of a-Si:H films lowers the energy barrier for hydrogen release, and the effect is more pronounced for *p*-type than *n*-type doping. This phenomenon can be explained by the lowered Si-H bond rupture energy when the Fermi level moves away from the middle of the bandgap.[11,12,14] A lower Si-H bond rupture energy will also result in enhanced diffusion and lowered free energy of desorption of H.[11] Furthermore, it has been shown that the presence of a doped capping layer may result in lowered Si-H bond rupture energy in the underlying intrinsic film.[13] This helps explain why a higher [H] was still incorporated into the bulk when the H_2 plasma treatment was conducted only on the a-Si:H(*i*) layer in the i/p^+ and i/n^+ stacks: the doped layers facilitate the release of this extra hydrogen.

The lowered energy barrier for H effusion in boron-doped a-Si:H(p^+) films has also been attributed in some studies to higher concentrations of voids.[11,12] More H atoms tend to be bound in dihydride (SiH_2) or higher hydrides in void-rich films, compared to monohydride (SiH) bonding in more compact films[21,29] and the Si-H bond energy is lower for SiH_2 than for SiH.[12,30] To determine the SiH_2/SiH ratio, FTIR measurements were conducted on Float-Zone (FZ) silicon wafers passivated with a-Si:H(*i*) layers, i/n^+ stacks, and i/p^+ stacks, with and without H_2 plasma treatment. The results are shown in Fig. 3. The thickness of the film/stack on each side was 40 nm, and, for the stacks, each component layer was 20 nm thick. The H_2 plasma treatment was conducted on the finished films or stacks. The FTIR absorption signal was fitted with a two-stretching-mode model to differentiate between SiH_2 and SiH.[21,29,31] The SiH_2/SiH ratio in a-Si:H(*i*) was increased by the H_2 plasma treatment, which is in agreement with Ref. 21. The results for the i/n^+ stack are similar to those for the a-Si:H(*i*) layer. The i/p^+ stack, on the other hand, already has a high SiH_2/SiH ratio before the H_2 plasma treatment, in accordance with the hypothesized void-rich and defective nature of boron-doped a-Si:H(p^+) films.[10] The H_2 plasma treatment did not increase the ratio to a higher level for the i/p^+ stack.

We have identified the origins of hydrogen in SHJ cells by measuring the regeneration rate of BO defects in lifetime samples made on UMG wafers with various structures and treatments. We conclude that the H_2 plasma treatment considerably increases [H] due to increased hydrogen concentration and SiH_2/SiH ratio in the a-Si:H films and that for [H] incorporation at $<250\,^{\circ}C$, the i/p^+ stack is more effective than the i/n^+ stack and both are more effective than intrinsic films alone due to the lowered Si-H bond rupture energy and higher SiH_2/SiH ratios. Therefore, the i/p^+ stack is beneficial for cells made on defect-rich silicon materials as it naturally enables bulk hydrogenation. We predict that an *n*-type hybrid cell structure with the i/p^+ stack on the rear and phosphorus-diffused n^+ layer in front can potentially achieve higher efficiencies. It avoids the parasitic absorption in normal SHJ cells and naturally combines the benefits of bulk hydrogenation and phosphorus gettering. A similar structure can also be designed for *p*-type substrates.

This work was supported by the Australian Renewable Energy Agency (ARENA) projects RND 005 and 1-A060, the Australian Centre for Advanced Photovoltaics (ACAP), and the U.S. National Science Foundation and Department of Energy under NSF Cooperative Agreement No. EEC-1041895. Apollon Solar is gratefully acknowledged for the supply of UMG silicon wafers. The authors would like to thank Dr. Sachin Surve for the help with sample preparations.

REFERENCES

[1]J. I. Hanoka, *Hydrogen in Disordered and Amorphous Solids* (Springer, 1986), p. 81.
[2]S. Pearton, J. Corbett, and T. Shi, Appl. Phys. A **43**, 153 (1987).
[3]C. Dube and J. I. Hanoka, "Hydrogen passivation of multicrystalline silicon," in Conference Record of the Thirty-First IEEE Photovoltaic Specialists Conference, Lake Buena Vista, FL, USA (2005).
[4]B. Hallam, C. Chan, M. Abbott, and S. Wenham, Sol. Energy Mater. Sol. Cells **141**, 125 (2015).
[5]B. Hallam, D. Chen, J. Shi, R. Einhaus, Z. C. Holman, and S. Wenham, Sol. RRL **2**, 1700221 (2018); Energy Mater. Sol. Cells **141**, 125 (2015).

[6]R. Basnet, F. E. Rougieux, C. Sun, S. P. Phang, C. Samundsett, R. Einhaus, J. Degoulange, and D. Macdonald, IEEE J. Photovoltaics **4**, 990 (2018).
[7]K. A. Münzer, "Hydrogenated silicon nitride for regeneration of light induced degradation," in Proceedings of the 24th EU-PVSEC, Hamburg, Germany (2009), p. 1558.
[8]G. Krugel, W. Wolke, J. Geilker, S. Rein, and R. Preu, Energy Procedia **8**, 47 (2011).
[9]C. Sun, D. Chen, W. Weigand, R. Basnet, S. P. Phang, B. Hallam, Z. C. Holman, and D. Macdonald, Appl. Phys. Lett. **113**, 152105 (2018).
[10]W. Beyer and H. Wagner, J. Phys. Colloq. **42**, C4-783 (1981).
[11]W. Beyer, J. Herion, and H. Wagner, J. Non-Cryst. Solids **114**, 217 (1989).
[12]W. Beyer, Physica B **170**, 105 (1991).
[13]S. De Wolf and M. Kondo, Appl. Phys. Lett. **91**, 112109 (2007).
[14]S. De Wolf and M. Kondo, J. Appl. Phys. **105**, 103707 (2009).
[15]N. Nampalli, B. Hallam, C. Chan, M. Abbott, and S. Wenham, Appl. Phys. Lett. **106**, 173501 (2015).
[16]S. Wilking, C. Beckh, S. Ebert, A. Herguth, and G. Hahn, Sol. Energy Mater. Sol. Cells **131**, 2 (2014).
[17]S. Wilking, S. Ebert, A. Herguth, and G. Hahn, J. Appl. Phys. **114**, 194512 (2013).
[18]S. Wilking, A. Herguth, and G. Hahn, J. Appl. Phys. **113**, 194503 (2013).
[19]B. Lim, "Boron–oxygen-related recombination centers in crystalline silicon and the effects of dopant-compensation," Ph.D. thesis (University of Hannover, 2012).
[20]R. Einhaus, J. Kraiem, B. Drevet, F. Cocco, N. Enjalbert, S. Dubois, D. Camel, D. Grosset-Bourbange, D. Pelletier, and T. Margaria, Photovoltaics Int. **9**, 60 (2010).
[21]A. Descoeudres, L. Barraud, S. De Wolf, B. Strahm, D. Lachenal, C. Guérin, Z. Holman, F. Zicarelli, B. Demaurex, and J. Seif, Appl. Phys. Lett. **99**, 123506 (2011).
[22]A. Herguth, Energy Procedia **124**, 53 (2017).
[23]F. Schindler, M. C. Schubert, A. Kimmerle, J. Broisch, S. Rein, W. Kwapil, and W. Warta, Sol. Energy Mater. Sol. Cells **106**, 31 (2012).
[24]D. Sperber, A. Graf, D. Skorka, A. Herguth, and G. Hahn, IEEE J. Photovoltaics **7**, 1627 (2017).
[25]C. Sun, D. Chen, F. Rougieux, R. Basnet, B. Hallam, and D. Macdonald, Sol. Energy Mater. Sol. Cells **195**, 174 (2019).
[26]A. Herguth, G. Schubert, M. Käs, and G. Hahn, Prog. Photovoltaics: Res. Appl. **16**, 135 (2008).
[27]B. Lim, F. Rougieux, D. Macdonald, K. Bothe, and J. Schmidt, J. Appl. Phys. **108**, 103722 (2010).
[28]S. Wilking, S. Ebert, C. Beckh, A. Herguth, and G. Hahn, "Of apples and oranges: Why comparing BO regeneration rates requires injection level correction," in 32nd European Photovoltaic Solar Energy Conference and Exhibition (2016), pp. 487–494.
[29]A. Smets, W. Kessels, and M. Van de Sanden, Appl. Phys. Lett. **82**, 1547 (2003).
[30]P. Gupta, V. Colvin, and S. George, Phys. Rev. B **37**, 8234 (1988).
[31]J. C. Knights, G. Lucovsky, and R. Nemanich, J. Non-Cryst. Solids **32**, 393 (1979).